WIRELESS COMMUNICATIONS AND MOBILE COMPUTING
Wirel. Commun. Mob. Comput. (2009)
Published online in Wiley InterScience
(www.interscience.wiley.com) DOI: 10.1002/wcm.746

Power distribution methods for MIMO-OFDM systems and field experimentations

Wladimir Bocquet[1*,†], Kazunori Hayashi[2] and Hideaki Sakai[2]

[1]*Orange Labs Tokyo, France Telecom Japan, Japan*
[2]*Graduate School of Informatics, Kyoto University, Japan*

Summary

In this paper, we propose several power allocation schemes for multi-input multi-output (MIMO) orthogonal frequency division multiplexing (OFDM) transmission based on the minimization of an approximated bit error rate (BER) expression, and we evaluate the different solutions *via* field trial experimentations. The methods illustrated in this paper, serve to allocate power among the different transmit antennas and the different subcarriers which compose the MIMO OFDM transmitted signal. Several solutions are available to perform power allocation. Frequency domain power allocation, spatial domain power allocation and combined spatial and frequency power allocation are evaluated. We first review and describe the analytical solution for each power allocation scheme and then evaluate the complexity in terms of both computational operations and BER performances. Simulation results show the performance in term of BER and link the advantage of each possibility of power distribution with the associated complexity. Copyright © 2009 John Wiley & Sons, Ltd.

KEY WORDS: power allocation; subcarrier grouping and field experimentation

1. Introduction

The growing demand for multimedia services and the growth of broadband Internet-related content has led to an increasing interest in high speed communications. This is because higher bit rate and higher quality applications such as intensive downloading or high quality streaming videos must be provided *via* the Internet. On the other hand, the requirements of increasingly wide bandwidth force the use of efficient transmission methods that would fit well to the characteristics of wideband channels especially in hostile multipath wireless environment where the signal propagates from transmitter to receiver along a number of different paths [1]. While propagating the signal power drops due to three effects: path loss, macroscopic and microscopic fading. Fading of the signal can be mitigated by different diversity techniques. In recent years, interest in the realization of high data rate wireless communication systems such as wireless local area networks (LANs) has been increasing. Among the IEEE 802.11 wireless

*Correspondence to: Wladimir Bocquet, Department of Network and Access, Orange Labs Tokyo, France Telecom Japan, Oiwake Bldg 9F, 3-1-13 Shinjuku, Shinjuku-ku, Tokyo 160-0022, Japan.
†E-mail: wladimir.bocquet@orange-ftgroup.com

LAN standards, 802.11a [2] and 802.11g [3] systems employ orthogonal frequency division multiplexing (OFDM), which offers high spectral efficiency and superior tolerance to multi-path fading. Another trend is the interest in the field of multi-antenna processing techniques. In a rich multipath environment, space division multiplexing (SDM) [4] with multi-input multi-output (MIMO) systems [5] can increase the transmission rate and has enormous communication capacity because of its spectral efficiency. Therefore, combining OFDM and SDM techniques [1] is a highly promising approach to realizing high data-rate wireless communications [6]. For power allocation among subcarriers in OFDM transmission, the Chow's algorithm [7] uses a criterion of minimizing the packet error rate while attaining a certain transmission rate, which also requires a complex iterative process. Another solution that consists of maximizing the spectral efficiency is another way to optimize the transmission performance [8–10]. In Reference [8], the water-filling method is used to allocate power in order to maximize the system capacity. In Reference [9], a multilevel transmit power scheme is proposed for OFDM with adaptive modulation.

In Reference [11], the authors propose a power allocation scheme for single-input single-output (SISO) OFDM based on an approximated expression of the bit error rate (BER), where the proposed subcarrier grouping method enables us to decrease the computational complexity with limited performance degradation. In this paper, we extend the method to MIMO-OFDM systems and propose three different power allocation schemes including frequency domain power allocation, spatial domain power allocation and combined spatial and frequency domains power allocation. Simplicity of the BER expression allows us to obtain a closed-form expression for the different power allocation strategies. The proposed power allocation methods using the subcarrier grouping scheme also allow us to control the balance between the transmission performance and the computational complexity by adjusting the size of the subcarrier group. Moreover, we evaluate, in a field trial experimentation, the different solutions and we show significant improvements of BER performance for the combined frequency and spatial domains-based power allocation scheme.

The rest of the paper is organized as follows. In Section 2, we review the conventional MIMO-OFDM scheme. In Section 3, we introduce the estimate value of BER for a channel encoded sequence and we describe in detail, in Section 4, the different power allocation schemes. In Section 5, we evaluate the computational complexity of the different power allocation methods and Section 6 gives the experimental results over QPSK and QAM modulations. Finally, conclusions are drawn in Section 7.

2. System Description

2.1. MIMO-OFDM Transceiver

The principle of OFDM transmission scheme [12] is to reduce the bit rate of each subcarrier and also to provide high bit rate transmission by using multiple low bit rate subcarriers. OFDM systems [13] can provide immunity against frequency selective fading because each carrier goes through non-frequency selective fading. At the transmitter part, the MIMO-OFDM scheme consists of N_t transmit (TX) and N_r receive (RX) antennas, denoted as an $N_t \times N_r$ system, where the transmitter sends an N_t-dimensional complex vector and the receiver receives an N_r-dimensional complex vector [14]. To combat inter symbol interference (ISI) and inter carrier interference (ICI), a guard interval (GI) [15] such as cyclic prefix (CP) or zero padding (ZP) is added to the OFDM symbols. At the receiver, we assume that the system is operating in a frequency selective Rayleigh fading environment [16] and the communication channel remains constant during transmission of one data frame. One data frame is composed of several MIMO-OFDM symbols and is assumed to be transmitted within the coherence time of the wireless system. In this case, channel characteristics remain constant during one frame transmission and may change between consecutive frame transmissions. We suppose that the fading channel can be modelled by a discrete-time baseband equivalent $(L-1)$th order finite impulse response (FIR) filter where L represents the time sample corresponding to the maximum delay spread. When the maximum delay spread does not exceed the GI, ISI does not occur on the MIMO-OFDM symbols, so the frequency domain MIMO-OFDM received signal after removal of GI is described by

$$y_{i,m}^{(q)} = \sum_{l=0}^{N_t-1} h_m^{(q,l)} \cdot \sqrt{p_{l,m}} \cdot x_{i,m}^{(l)} + n_{i,m}^{(q)} \qquad (1)$$

where $y_{j,m}^{(q)}$ is the received signal at the qth received antenna for the ith OFDM symbol and the mth subcarrier and $h_m^{(q,l)}$ is the channel frequency response

DOI: 10.1002/wcm

on the mth subcarrier from the lth transmitting antenna to the qth receiving antenna which composes a MIMO channel matrix. Furthermore, $x_{i,m}^{(l)}$ and $p_{l,m}$ are respectively the modulated data symbol and the transmit power on the lth transmit antenna for the ith OFDM symbol on the mth subcarrier. In addition, $n_{j,m}^{(q)}$ denotes zero mean additive white Gaussian noise (AWGN) with N_r independent and identically distributed (iid), complex elements for the qth received antenna [16,17].

2.2. Linear Detection for MIMO-OFDM Scheme

In this paper, we focus as the linear detection scheme. Thus, output of the compensation scheme can be described by

$$\mathbf{z}_{i,m} = \mathbf{G}_m \cdot \mathbf{y}_{i,m} \tag{2}$$

where $\mathbf{z}_{i,m} = [z_{i,m}^{(0)}, \cdots, z_{i,m}^{(N_\mathrm{t}-1)}]^\mathrm{T}$ and $\mathbf{y}_{i,m} = [y_{i,m}^{(0)}, \cdots, y_{i,m}^{(N_\mathrm{r}-1)}]^\mathrm{T}$, respectively denote the output of the equalizer and the received signal. In the case of zero forcing (ZF) detection [14], the equalizer matrix is calculated as

$$\mathbf{G}_m = (\mathbf{H}_m^H \mathbf{H}_m)^{-1} \cdot \mathbf{H}_m^H \tag{3}$$

with

$$\mathbf{G}_m = \begin{bmatrix} g_m^{(0,0)} & \cdots & g_m^{(0,N_\mathrm{r}-1)} \\ \cdot & \cdots & \cdot \\ \cdot & \cdots & \cdot \\ g_m^{(N_\mathrm{t}-1,0)} & \cdots & g_m^{(N_\mathrm{t}-1,N_\mathrm{r}-1)} \end{bmatrix} \tag{4}$$

and

$$\mathbf{H}_m = \begin{bmatrix} h_m^{(0,0)} & \cdots & h_m^{(0,N_\mathrm{t}-1)} \\ \cdot & \cdots & \cdot \\ \cdot & \cdots & \cdot \\ h_m^{(N_\mathrm{r}-1,0)} & \cdots & h_m^{(N_\mathrm{r}-1,N_\mathrm{t}-1)} \end{bmatrix} \tag{5}$$

3. Bit Error Rate Expression

3.1. Channel Coding

We utilize an approximated BER expression based on convolutional coded (CC) [2,3] data transmission. The generator polynomial of the mother code is $g = [133, 171]$ of rate $R = 1/2$ and $K = 7$ and the other coding rates ($R = 3/4$ and $R = 2/3$) are obtained from the puncturing pattern described in the WLAN based channel coding. At the receiver, the soft output Viterbi algorithm (SOVA) is performed to recover the original sequence [18].

3.2. Approximated BER Expression

In the AWGN channel, considering the performance of QPSK and QAM modulations, the BER is shown to be well approximated by [19]

$$\mathrm{BER} \approx 0.2 \cdot \exp\left\{-1.5 \cdot \frac{\gamma}{(N_m - 1)}\right\} \tag{6}$$

for $0 \le \gamma < 30\,\mathrm{dB}$ where γ is the SNR and N_m is the number of bits per symbol ($N_m = 2$ for QPSK, $N_m = 4$ for 16-QAM and $N_m = 6$ for 64-QAM).

By extension to the Rayleigh Fading channel case [20], we can derive the performance of QPSK and QAM modulations. Let $\overline{\gamma}$ and $\overline{\mathrm{BER}}$ denote the average SNR and BER, respectively. The probability density function of the instantaneous SNR γ is given, for $\gamma > 0$ by

$$p(\gamma) = \frac{1}{\overline{\gamma}} \cdot \exp\left\{-\frac{\gamma}{\overline{\gamma}}\right\} \tag{7}$$

The average BER, $\overline{BER}$, is evaluated as

$$\overline{\mathrm{BER}} \approx \int_0^\infty 0.2 \cdot \exp\left\{-1.5 \cdot \frac{\gamma}{(M-1)}\right\} \cdot \frac{1}{\overline{\gamma}} \cdot \exp\left\{-\frac{\gamma}{\overline{\gamma}}\right\} \mathrm{d}\gamma \tag{8}$$

and the previous approximation can be bound as [21] and [22]

$$\mathrm{BER} \le a \cdot \exp\left\{-b \cdot \frac{\gamma}{(M-1)}\right\} \tag{9}$$

Therefore, we will use this heuristic approximation to evaluate the power allocation scheme and then we adjust the BER approximation based on computer matching. The approximation can be expressed as

$$f(\beta_{l,m}, p_{l,m}) \approx a \cdot \exp\left\{-b \cdot \beta_{l,m} \cdot p_{l,m}\right\} \tag{10}$$

DOI: 10.1002/wcm

Table I. Transmission modes for coding rate $R = 1$.

Modulation	QPSK	16-QAM	64-QAM
a	0.2	0.2	0.15
b	1.66	1.73	1.68

Table II. Transmission modes for coding rate $R = 1/2$.

Modulation	QPSK	16-QAM	64-QAM
a	7.0	4.0	1.5
b	9.5	11.0	12.0

where $\beta_{l,m}$ is equal to

$$\beta_{l,m} = \frac{1}{(2^{N_m} - 1) \cdot \sigma_n^2 \cdot \sum_{n=0}^{N_r - 1} |g_m^{(l,n)}|^2} \tag{11}$$

where σ_n^2 denotes the variance of the AWGN and $\beta_{l,m}$ denotes the received signal-to-noise ratio (SNR), which depends on the modulation scheme and the equalizer weights on the mth subcarrier and lth transmit antenna. $p_{l,m}$ denotes the transmit power mth subcarrier and lth transmit antenna. The parameters a and b are to be determined in a heuristic way, namely, *via* computer simulations.

Tables I and II summarize the parameters of a and b for QPSK, 16-QAM and 64-QAM, without channel coding and with channel coding $R = 1/2$, obtained *via* computer simulations.

In the rest of the paper, we will detail process to evaluate the transmit power, denoted $p_{l,m}$, based on the minimization of the BER expression described by $f(\beta_{l,m}, p_{l,m})$ for known value of $\beta_{l,m}$.

In the rest of the paper, we will detail process to evaluate the transmit power, denoted $p_{l,m}$, based on the minimization of the BER expression described by $f(\beta_{l,m}, p_{l,m})$ for known value of $\beta_{l,m}$.

4. Power Allocation Scheme

The proposed scheme is based on a procedure which consists of optimizing the transmit power in terms of the expression of the approximated BER under power constraint and considering the subcarrier grouping scheme for frequency domain-based power allocation. We next review the possible strategies to allocate power for both optimal and suboptimal solutions.

First, let the matrix representation of transmit power be defined as

$$\mathbf{p}'_o = \begin{bmatrix} p'_{0,0,\mathbf{o}} & \cdots & p'_{0,N-1,\mathbf{o}} \\ \cdot & \cdots & \cdot \\ \cdot & \cdots & \cdot \\ p'_{N_t-1,0,\mathbf{o}} & \cdots & p'_{N_t-1,N-1,\mathbf{o}} \end{bmatrix} \tag{12}$$

In this paper, we consider power distribution with the condition that the average transmit power per symbol is kept constant to be $\overline{P}$.

4.1. Combined Spatial and Frequency Domains Power Allocation

The basic principle of the combined spatial and frequency domain power allocation for a MIMO-OFDM signal is to combine spatial and frequency domain optimization [23] of the transmit power as a function of the heuristic BER expression [24] defined in Equation (10). The Lagrangian optimization method will be used to obtain an analytical value of the power allocation for each load subcarrier. Furthermore, a constraint is added in order to keep the global transmit power at the transmitter constant. The optimal case is to consider the power allocation scheme through one MIMO-OFDM symbol which is represented by $(N \cdot N_t)$ elements. However, due to the computation complexity to perform this power allocation scheme, we propose to perform it through a limited number of N_s subcarriers and then repeat the allocation scheme N/N_s times.

Let us first define the proposed transmit power matrix of the tth subcarrier group as

$$\mathbf{p}'^{(t)}_o = \begin{bmatrix} p'_{0,t\cdot N_s,\mathbf{o}} & \cdots & p'_{0,(t+1)\cdot N_s-1,\mathbf{o}} \\ \cdot & \cdots & \cdot \\ \cdot & \cdots & \cdot \\ p'_{N_t-1,t\cdot N_s,\mathbf{o}} & \cdots & p'_{N_t-1(t+1)\cdot N_s-1,\mathbf{o}} \end{bmatrix} \tag{13}$$

with

$$\boldsymbol{\beta}'^{(t)} = \begin{bmatrix} \beta'_{t\cdot N_s} & \cdots & \beta'_{t\cdot N_s+N_s-1} \end{bmatrix}^{\mathrm{T}} \tag{14}$$

where $\boldsymbol{\beta}'^{(t)}$ denotes the tth, $(t = 0, \cdots, N/N_s - 1)$, group of the elements represented by Equation (9).

DOI: 10.1002/wcm

Then, the optimization problem can be stated as

$$\begin{cases} \mathbf{p}_{\mathbf{o}}^{\prime(t)} = \arg\min \sum_{l=0}^{N_t-1} \sum_{m=0}^{N_s-1} \frac{f(\beta'_{l,t\cdot N_s+m}, p'_{l,t\cdot N_s+m})}{N_s \cdot N_t} \\ \text{s.t.} \sum_{l=0}^{N_t-1} \sum_{m=0}^{N_s-1} p'_{l,t\cdot N_s+m} = N_s \cdot N_t \cdot \overline{P} \end{cases} \tag{15}$$

One possibility to solve this optimization problem is to apply the Lagrangian procedure. Defining

$$J(\mathbf{p}_{\mathbf{o}}^{\prime(t)}) = \sum_{l=0}^{N_t-1} \sum_{m=0}^{N_s-1} \frac{f(\beta_{l,t\cdot N_s+m}, p_{l,t\cdot N_s+m})}{N_t \cdot N_s} + \lambda \cdot \left(\sum_{l=0}^{N_t-1} \sum_{m=0}^{N_s-1} p_{l,t\cdot N_s+m} - N_t \cdot N_s \cdot \overline{P} \right) \tag{16}$$

The optimal solutions are obtained by solving for $0 \leq l < N_t$ and $0 \leq m < N_s$

$$\begin{cases} \frac{\partial}{\partial p_{l,m}} \left(\sum_{l=0}^{N_t-1} \sum_{m=0}^{N_s-1} \frac{f(\beta_{l,t\cdot N_s+m}, p_{l,t\cdot N_s+m})}{N_t \cdot N_s} \right) + \lambda = 0 \\ \sum_{l=0}^{N_t-1} \sum_{m=0}^{N_s-1} p_{l,t\cdot N_s+m} - N_t \cdot N_s \cdot \overline{P} = 0 \end{cases} \tag{17}$$

After calculation and rearrangement for $0 \leq l < N_t$ and $0 \leq m < N_s$, we obtain

$$p_{l,t\cdot N_s+m,\mathbf{o}} = \left[\sum_{u=0}^{N_t-1} \sum_{v=0}^{N_s-1} \frac{\beta_{l,t\cdot N_s+m}}{\beta_{u,t\cdot N_s+v}} \right]^{-1} \cdot \left[N_t \cdot N_s \cdot \overline{P} + \frac{1}{b} \cdot \sum_{u=0}^{N_t-1} \sum_{v=0}^{N_s-1} \frac{1}{\beta_{u,t\cdot N_s+v}} \cdot \log\left(\frac{\beta_{l,t\cdot N_s+m}}{\beta_{u,t\cdot N_s+v}} \right) \right] \tag{18}$$

We repeat the power allocation process for each subset of subcarriers and transmit antennas which compose the MIMO-OFDM symbol and each transmit antenna.

Moreover, contrary to the rank adaption scheme, the proposed scheme tends to allocate more power to the subcarriers that are strongly affected by channel fading. The proposed solution tends to flatten the channel variation, so that uniform coding scheme between the different subcarrier is possible and appropriate.

4.2. Combined Spatial and Frequency Domain Power Allocation for Uncoded Channel Case with Exact BER Expression and Maximum Group Size

In the case of uncoded system (i.e. without any channel encoder), it is possible to exactly evaluate the BER performance for both QPSK and QAM modulations. It is well-known that the BER expression is a function of the Q-function [16] defined by $Q(x) \doteq (1/\sqrt{2\pi}) \int_x^\infty \exp(-t^2/2)\mathrm{d}t$. However, optimization problem which consists of minimizing the exact BER expression under a power constraint cannot be solved analytically. The optimization problem is stated as

$$\begin{cases} \mathbf{p}_{\text{exact}}^{\prime(t)} = \arg\min \sum_{l=0}^{N_t-1} \sum_{m=0}^{N-1} \frac{Q(\beta'_{l,m}, p'_{l,m})}{N \cdot N_t} \\ \text{s.t.} \sum_{l=0}^{N_t-1} \sum_{m=0}^{N-1} p'_{l,m} = N \cdot N_t \cdot \overline{P} \end{cases} \tag{19}$$

Nevertheless, by an using iterative algorithm such as the steepest-descent method [25], the optimization problem can be solved.

4.3. Spatial Domain Power Allocation Scheme

For the specific case of spatial domain power allocation, the optimization problem described in Equation (19) can be simplified [26] and described for $0 \leq m < N$ as

$$\begin{cases} \mathbf{p}_{\mathbf{o}}^{\prime(t)} = \arg\min \sum_{l=0}^{N_t-1} \frac{f(\beta'_{l,m}, p'_{l,m})}{N_t} \\ \text{s.t.} \sum_{l=0}^{N_t-1} p'_{l,m} = N_t \cdot \overline{P} \end{cases} \tag{20}$$

Then, after some calculations and similar rearrangements presented in Section 4.1, we obtain the following solution for $0 \leq m < N$

$$p_{l,m} = \left[1 + \sum_{\substack{u=0 \\ u \neq l}}^{N_t-1} \frac{\beta_{l,m}}{\beta_{u,m}} \right]^{-1} \times \left[N_t . \overline{P}_m + \frac{1}{b} \times \sum_{\substack{u=0 \\ u \neq l}}^{N_t-1} \frac{1}{\beta_{u,m}} \times \log\left(\frac{\beta_{l,m}}{\beta_{u,m}} \right) \right] \tag{21}$$

DOI: 10.1002/wcm

4.4. Frequency Domain Power Allocation Scheme

Without considering the spatial freedom axis, the optimization problem, described in Equation (19), can be restricted to the frequency domain. Then, the problem description is, for $0 \leq l < N_t$, equal to

$$\begin{cases} \mathbf{p_o}'^{(t)} = \arg\min \sum_{m=0}^{N_s-1} \frac{f(\beta'_{l,t\cdot N_s+m}, p'_{l,t\cdot N_s+m})}{N_s} \\ \text{s.t.} \sum_{m=0}^{N_s-1} p'_{l,t\cdot N_s+m} = N_s \cdot \overline{P} \end{cases} \quad (22)$$

We solve the optimization problem by performing the Lagrange multiplier using similar rearrangements as presented in Section 4.1. The closed form optimal solution is obtained, for $0 \leq l < N_t$, as

$$p'_{l,t\cdot N_s+m,so} = \left[\sum_{u=0}^{N_s-1} \frac{\beta'_{l,t\cdot N_s+m}}{\beta'_{l,t\cdot N_s+u}}\right]^{-1} \cdot \left[N_s\overline{P} + \sum_{u=0}^{N_s-1} \frac{1}{\beta'_{l,t\cdot N_s+u}\cdot b} \log\left(\frac{\beta'_{l,t\cdot N_s+m}}{\beta'_{l,t\cdot N_s+u}}\right)\right] \quad (23)$$

5. Computational Complexity

The main advantages of the proposed scheme are both the simplicity compared to any iterative algorithms such as steepest decent and the low additional complexity compared to the suboptimal solution which does not include the knowledge of the channel condition in the power allocation process. Complexity of the steepest descent algorithm [27] is basically equal to $O(N_s^2)$ per iteration. In addition, the power allocation process needs to be repeated N/N_s times (for simplicity, we assume that N/N_s is an integer). The analytical part of the calculation that is performed for the estimation of the power allocation is equal to $O(U \cdot \text{Log}(U))$, where U denotes the number of elements that compose the group size. In the case of the spatial power allocation scheme, the complexity per MIMO-OFDM symbol is equal to $O(N \cdot N_t \cdot \text{Log}(N_t))$. For the frequency domain power distribution scheme, the complexity becomes equal to $O(N/N_s \cdot N_t \cdot N_s \cdot \text{Log}(N_s))$. Finally, for the combined frequency and spatial domain power allocation scheme, the complexity is equivalent to $O(N/N_s \cdot N_t \cdot N_s \cdot \text{Log}(N_t \cdot N_s))$. In addition, the main advantage of the proposed scheme is the simplicity compared to iterative algorithms such as the steepest decent on the exact expression of the BER. Complexity of the steepest descent algorithm is basically equal to $O(N/N_s \cdot N_t \cdot N_s^3)$.

6. Simulation Results

6.1. Software Simulation

We now evaluate the performance of the proposed power allocation method for MIMO-OFDM scheme in a multi-path fading environment with ZF detection. We assume, as described in Table III, perfect knowledge of the channel variations both at the transmitting and receiving parts. An exponentially decaying (1-dB decay) multi-path model is assumed and the carrier frequency is equal to 2.4 GHz. The IFFT/FFT size is 64 points and the GI is set to 16 samples [3].

The effect of the combined frequency and spatial domain power allocation scheme for several subset sizes is highlighted for the specific antenna configuration $N_t = N_r = 4$ for QPSK and QAM modulations.

Figures 1–3 show the BER *versus* the total received SNR (dB) for the proposed scheme with various subcarrier group sizes N_s without channel encoder $R = 1$. The BER performance of the conventional scheme (equal power distribution) is also plotted in the same figure.

The simulation results in Figure 1 shows that for QPSK modulation at average BER $= 10^{-4}$, 2.8, 4.5, 5.2, 6.1 and 8.7 dB gains are obtained respectively for $N_s = 2$, 4, 8, 16 and 64. For reference, we have plotted the performance of the exact BER expression with steepest descent algorithm for the case $N_s = 64$. At average BER $= 10^{-4}$, the difference between the

Table III. Simulation parameters.

Carrier frequency	2.4 GHz
Bandwidth	20 MHz
(N_t, N_r)	(2,2), (4,4)
Modulations	QPSK, 16-QAM, 64-QAM
Channel encoder	No code and convolutional code
Coding gain	$R = 1/2$ and 1
Channel estimation	Perfect CSI
Number of data subcarrier	64
Guard interval length	16
Channel model	5-path, Rayleigh fading
Sample period	0.05 μs
Number of data packet	20
Subgroup size (N_s)	2, 4, 8, 16, 32, 64

DOI: 10.1002/wcm

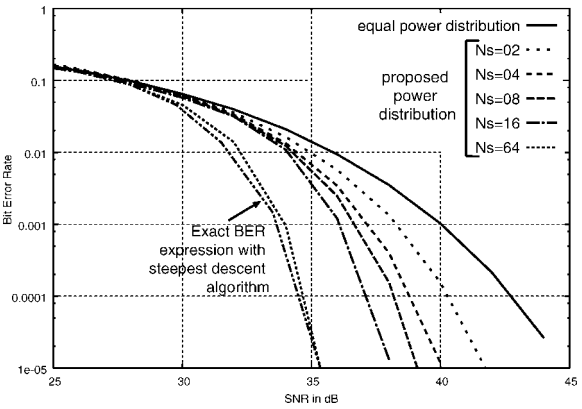

Fig. 1. Bit error rate performance for QPSK modulation and coding rate $R = 1$.

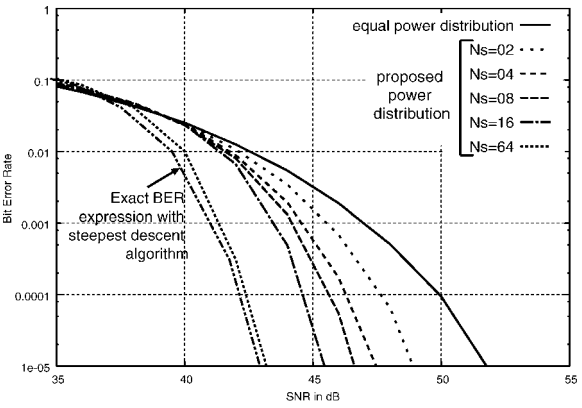

Fig. 2. Bit error rate performance for 16-QAM modulation and coding rate $R = 1$.

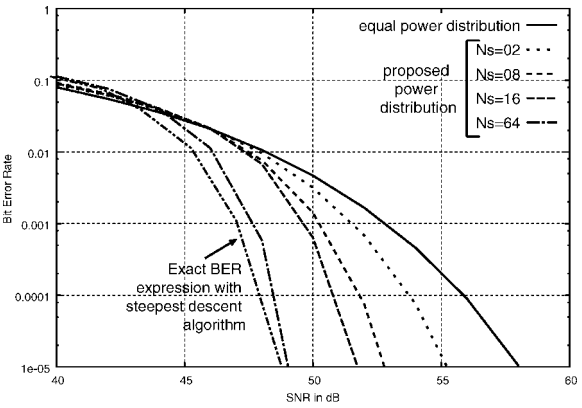

Fig. 3. Bit error rate performance for 64-QAM modulation and coding rate $R = 1$.

proposed suboptimum scheme and the optimum case is less than 0.6 dB.

Figures 2 and 3 show the BER performance with 16- and 64-QAM modulations, respectively for several subcarrier group sizes. From these figures, we can see that the proposed scheme can achieve significant performance gain also for QAM modulation.

In Figures 4–6, the benefit of performing the proposed scheme, in function of the total received SNR, is highlighted for the specific case of $R = 1/2$, $N_t = N_r = 4$, and QPSK and 64-QAM modulations. The simulation results show that at average BER $= 10^{-4}$, between 2.5 and 6 dB gains are obtained depending on the subcarrier grouping size (N_s =2, 4 and 64) for QPSK modulation. In the case of 16- and 64-QAM modulations, the proposed power allocation with ordering allows to obtain between 2.5 and 7 dB gain depending on the size of the subcarrier grouping, N_s. The benefit in term of gain for QAM modulation is comparable to the QPSK modulation.

It is shown that the subcarrier grouping size strongly affects the performance of the proposed scheme for both QPSK and QAM modulations. However, due

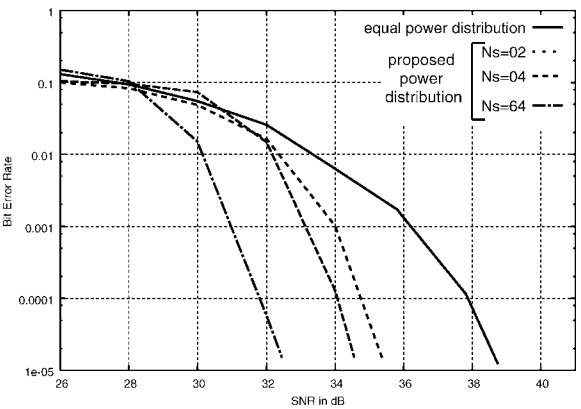

Fig. 4. Bit error rate performance for QPSK modulation and coding rate $R = 1/2$.

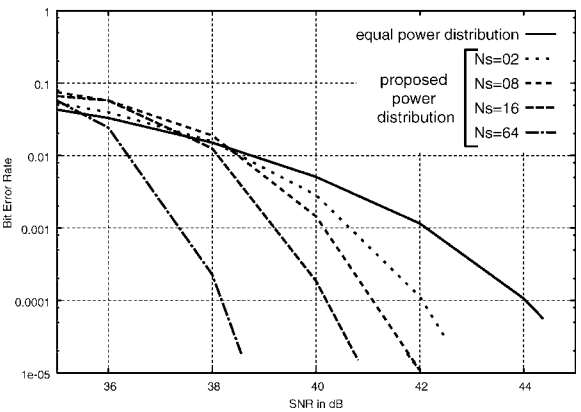

Fig. 5. Bit error rate performance for 16-QAM modulation and coding rate $R = 1/2$.

DOI: 10.1002/wcm

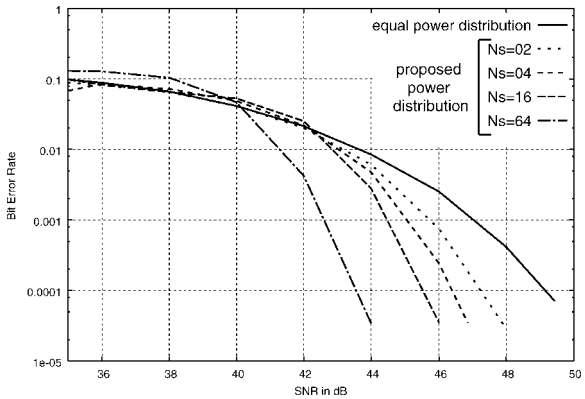

Fig. 6. Bit error rate performance for 64-QAM modulation and coding rate $R = 1/2$.

to the structure of the proposed power distribution scheme, there is a trade-off between the subcarrier grouping size and the computational complexity.

Restrictions regarding the FCC requirements are not considered, at the present time, in the simulation results and experimentations. The objectives of this study is to highlight the possibility of power allocation-based schemes for future mobile communication.

6.2. Field Experimentation

We now evaluate the performance of the different power allocation methods for the MIMO-OFDM system in a real environment. System parameters are shown in Table IV. The main system parameters are based on the IEEE 802.11a standard with time division multiplexing for pilot structure. In addition, a Viterbi algorithm is included to decode the received signal. Experimentation was carried out in an indoor environment and the channel was considered quasi-static during one frame transmission [28]. Channel 3 in the 5 GHz frequency band ($F_c = 5210$ MHz) was used to transmit data and to evaluate the channel response. Furthermore, off-line processing was performed to extract the channel gains and delay for each significant

Table IV. Simulation parameters.

Carrier frequency	5.21 GHz
Bandwidth	20 MHz
Modulation scheme	QPSK, 16-QAM, 64-QAM
Channel encoder	Convolutional codes, $R = 1/2$
Number of data subcarrier	64
Guard interval length	16
Channel model	Real environment
Sample period	0.05 μs
Number of data packet	20

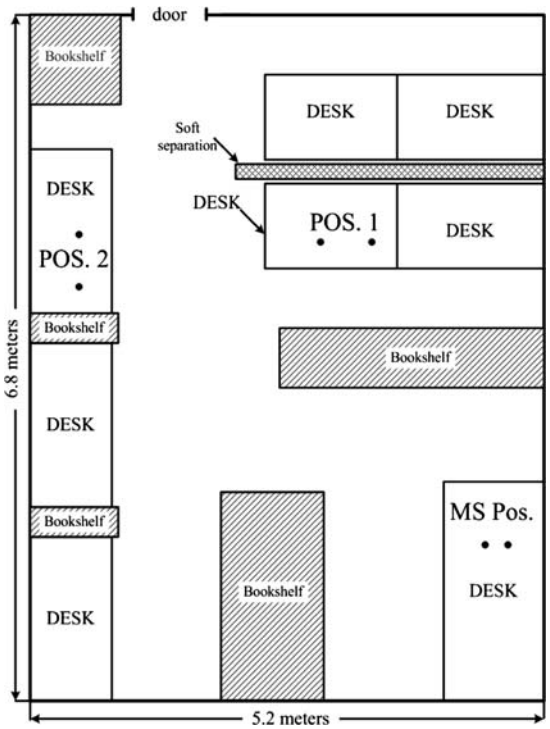

Fig. 7. Layout of the room.

path. The transmitter comprised two IEEE 802.11a WLAN cards and the separation between the antenna elements was equal to 6λ, where λ represents the carrier wavelength. The receiving part was composed of a two-element antenna and the adjacent spacing was equal to 3λ/2. Such spacing was employed since the mutual coupling influence is low at this distance [29]. In addition, the ZF detection scheme is employed in the receiver and the baseband processing is performed off-line for all the experimentations.

The focus of the field experimentation is to evaluate the different power allocation schemes in an indoor and quasi-static environment.

Figure 7 shows the layout of the room where experimentation was done and the different positions of the different antenna elements. The environment simulates a typical modern open office where several desks are set up in the same room.

6.2.1. Experimental results for position 1

Table V shows the average transmit SNR in dB for an average BER $= 10^{-5}$ in the case of channel coding $R = 1/2$ and several modulation schemes (i.e. QPSK, 16- and 64-QAM). For reference in the table, S domain, F domain and S+F domain, respectively

DOI: 10.1002/wcm

Table V. Average SNR (*dB*) for BER $= 10^{-5}$ at the position 1.

Modulation	QPSK	16-QAM	64-QAM
Equal power	30.5	35.4	37.5
S domain	29.8	35.0	37.2
F domain, $N_s = 2$	29.6	34.4	36.9
F domain, $N_s = 4$	28.9	34.1	36.5
F domain, $N_s = 8$	28.1	33.9	35.8
F domain, $N_s = 16$	27.1	33.0	35.0
S+F domains, $N_s = 2$	29.3	34.0	36.6
S+F domains, $N_s = 4$	28.4	33.75	36.3
S+F domains, $N_s = 8$	27.8	33.5	35.6
S+F domains, $N_s = 16$	26.6	32.6	34.7

denote spatial power allocation scheme described by Equation (21), frequency domain power allocation described in Equation (23) and combined spatial and frequency domain power distribution detailed in Equation (18). In addition, equal power denotes conventional transmission without any specific power allocation. As described in Table V, a gain of about 4 dB is obtained by simply performing the combined spatial and frequency domains power allocation scheme with $N_s = 16$, compared to the equal power distribution method for QPSK modulation. In the case of 16- and 64-QAM modulation, a gain of about 3 dB is obtained for the conditions described above. In the case of the power allocation scheme in the spatial domain, 0.7, 0.4 and 0.3 dB gains are obtained for QPSK, 16- and 64-QAM modulation, respectively. Furthermore, on average, 0.4 dB gain is obtained for the three different modulations (QPSK, 16-, 64-QAM) by extending the power allocation to both the spatial and frequency domains compared to the frequency domain only.

6.2.2. *Experimental results for position 2*

Table VI shows the average transmit SNR in dB for an average BER $= 10^{-5}$ in the case of channel coding $R = 1/2$ and several modulation schemes (i.e. QPSK, 16- and 64-QAM). In this table, the effect of the different power allocation schemes for several subset sizes is highlighted for the antenna configuration $N_t = N_r = 2$ at the position denoted 2 in Figure 7 for QPSK and QAM modulations.

Table VI. Average SNR (*dB*) for BER $= 10^{-5}$ at the position 2.

Modulation	QPSK	16-QAM	64-QAM
Equal power	30.3	33.4	36.9
S domain	30.0	33.1	36.6
F domain, $N_s = 2$	29.8	32.8	36.2
F domain, $N_s = 4$	29.0	33.2	35.6
F domains, $N_s = 8$	28.1	31.1	34.2
F domains, $N_s = 16$	27.0	29.9	32.9
S+F domain, $N_s = 2$	29.4	32.5	35.9
S+F domain, $N_s = 4$	28.8	31.8	35.2
S+F domains, $N_s = 8$	27.9	30.8	34.0
S+F domains, $N_s = 16$	26.7	29.6	32.4

For the QPSK modulation scheme, channel coding rate $R = 1/2$, the specific MIMO configuration $N_t = N_r = 2$ and various subcarrier group sizes N_s, the BER performances of the conventional scheme (equal power distribution) is also plotted in the same figure. According to the experimentations, at average BER $= 10^{-5}$, 0.3 dB gain is obtained for the spatial domain power allocation scheme compared to the conventional scheme. In the case of the frequency domain power allocation, respectively 0.5, 1.3, 2.1 and 3.1 dB gains are obtained for $N_s = 2$, $N_s = 4$, $N_s = 8$ and $N_s = 16$, compared to equal power distribution. For frequency and spatial domain power distribution, gains of 0.7, 1.6, 2.3 and 3.4 dB are obtained for $N_s = 2$, $N_s = 4$, $N_s = 8$ and $N_s = 16$, respectively, compared to equal power distribution. So, for QPSK modulation and $N_t = N_r = 2$, the main gain is obtained by the frequency domain power allocation for MIMO-OFDM transmission. Extension to the spatial domain allows an additional 0.3 dB gain compare to equal power distribution.

Table VI presents average transmit SNR in dB for an average BER $= 10^{-5}$ for the different power allocation schemes with QAM modulations too with various subcarrier group sizes N_s too. Similarly to the QPSK modulation, limited gain, about 1 dB is obtained, compared to equal power distribution, for spatial domain-based power allocation. Main additional gain is highlighted for the frequency domain power allocation and large number for N_s.

7. Conclusion

This paper proposes a field trial evaluation of power distribution for MIMO-OFDM transmission in a quasi-static multipath environment. It consists of adapting the transmit power in the spatial and/or frequency domain using a heuristic expression of the BER for each subcarrier. A review of the different power allocation strategies based on a closed-form expression of the optimum power to be allocated for each subcarrier is presented. In the case of the frequency based power allocation, it allows to reduce the computational complexity, by including a subcarrier grouping method with local power adaptation for each subcarrier

DOI: 10.1002/wcm

group. Our subcarrier grouping method minimizes the adverse impact of the local power adaptation by taking into consideration the channel gains of all the subcarriers. The characteristics allow us to control the trade-off between the transmission performance and the computational complexity by adjusting the sizes of subcarrier groups. The simulation results show significant improvement of BER performance both for QPSK and QAM modulation compared to the equal power allocation scheme. Furthermore, combining the proposed scheme to any powerful detection such as maximum likelihood detection (MLD) can be also implemented. In this paper, we have limited the channel coding scheme to the convolutional code. However, other powerful coding schemes such as the turbo codes (TC) [30] or low density parity check (LDPC) [31,32] can also be included in the modulated transmission. Finally, future orientation for this work would include the introduction of error in the channel estimation [33] and the extension of the experimentation in the outdoor environment with mobility. In the future, additional studies on FCC restrictions should be performed to emphasize the feasibility of our proposed solution. Additional restrictions on power constraints can be easily added to keep the system within the transmit power recommendations.

Acknowledgments

The authors thank Dr. Yukou Mochida and Mr. Jerome Laudouar of France Telecom R&D Tokyo for their valuable discussions and supports and Pr. Shinsuke Hara for the facility to perform measurements.

References

1. Sampath H, Talwar S, Tellado J, Erceg V, Paulraj A. A fourth-generation MIMO-OFDM broadband wireless system: design, performance and field trial results. *IEEE Commununications Magazine* 2002; **40**(9): 143–149.
2. IEEE 802.11a standard. ISO/IEC 8802-11, 1999.
3. Draft IEEE 802.11g standard. Further higher speed physical layer extension in the 2.4GHz band, 2001.
4. van Zelst A, van Nee R, Awater GA. Space division multiplexing (SDM) for OFDM systems. *IEEE VTC-Spring*, Tokyo, Japan, May 2000.
5. Foschini GJ, Golden GD, Valenzuela RA, *et al*. Simplified processing for high spectral efficiency wireless communication employing multi-element arrays. *IEEE Journal on Selected Areas of Communication* 1999; **17**(11): 1841–1852.
6. Li Y, Winters JH, Sollenberger NR. MIMO-OFDM for wireless communications: signal detection with enhanced channel estimation. *IEEE Transactions on Communication* **50**(9): 1471–1477.
7. Chow P, Cioffi J, Bingham J. A practical discrete multitone transceiver loading algorithm for data transmission over spectrally shaped channels. *IEEE Transactions on Communication* 1995; **43**(234): 773–775.
8. Yun W, Cioffi J. On constant power water-filling. In *Proceedings of IEEE International Conference on Communication, ICC'01*, June 2001.
9. Yoshiki T, Sampei S, Morinaga N. High bit rate transmission scheme with a multilevel transmit power control for OFDM based adaptive modulation systems. In *Proceedings of IEEE VTS Vehicular Technology Conference, VTC'01 Spring*, May 2001.
10. Falahati S, Svensson A, Sternad M, Ekman T. Adaptive modulation systems for predicted wireless channels. *IEEE Transaction on Communication* 2004; **52**(2): 307–316.
11. Bocquet W, Hayashi K, Sakai H. Frequency domain power adaptation scheme for coded OFDM transmissions. In *Proceeding of European Wireless*, Paris, France, April 2007.
12. Van Nee R, Prasad R. *OFDM for Wireless Multimedia Communications*. Artech House Publisher, 2000.
13. Cimini LJ. Analysis and simulation of digital mobile channel using orthogonal frequency division multiplexing. *IEEE Transactions on Commununication* 1985; **33**(7): 665–675.
14. Van Zelst A, *et al*. Implementation of a MIMO-OFDM-based wireless LAN system. *IEEE Transactions on Signal Processing* 2004; **52**(2): 483–494.
15. Muquet B, de Courvillel M, Giannakis GB, Wang Z, Duhamel P. Reduced complexity equalizers for zero-padded OFDM transmissions. In *Proceedings of IEEE International Conference on Acoustics, Speech, and Signal Processing (ICASSP'00)*, 2000; **5**: 2973–2976.
16. Proakis J. *Digital Communications* (3rd edn). McGraw-Hill: Singapore, 1995.
17. Biglieri E, Caire G, Taricco G. Limiting performance of block fading channels with multiple antennas. *IEEE Transactions on Information Theory* 2001; **47**: 1273–1289.
18. MacWilliams FJ, Sloane NJA. *The Theory of Error-correcting Codes*. North-Holland: New York, NY, 1977.
19. Alouini M-S, Goldsmith A. Adaptive modulation over Nakagami fading channels. *Kluwer Journal on Wireless Communications* 2000; **13**(1–2): 119–143.
20. Foschini GJ, Salz J. Digital communications over fading radio channels. *Bell System Technical Journal* 1983; 429–456.
21. Qiu X, Chawla K. On the performance of adaptive modulation in cellular system. *IEEE Transactions on Commununication* 1999; **47**(6): 884–895.
22. Liu Q, Zhou S, Giannakis G. Cross-layer comibining of adaptive modulation and coding with truncated ARQ over wireless links. *IEEE Transactions on Wireless Communication* 2004; **3**(5): 1746–1755.
23. Bocquet W, Hayashi K, Sakai H. Combined frequency and spatial domains power distribution for MIMO-OFDM transmission. In *IEEE PIMRC*, Athens, Greece, September 2007.
24. Jiang Zh, *et al*. Max-utility wireless resource management for best-effort traffic. *IEEE Wireless Commununications Magazine* 2005; **4**(1): 100–111.
25. Widrow B, Stearns SD. *Adaptive Signal Processing*. Prentice-Hall: Englewood Cliffs, NJ, 1985.
26. Bocquet W, Hayashi K, Sakai H. A power allocation scheme for MIMO-OFDM systems. In *IEEE ISCSSP*, Marakech, Morocco, March 2006 (invited paper).
27. Park CS, Lee KB. Transmit power allocation for BER performance improvement in multicarrier systems. *IEEE Transaction on Communication* 2004; **52**(10): 1658–1663.
28. Tran QT. A study on phased array antenna with RF-MEMS phase shifters. *Master Thesis*, Osaka University, February 2005.
29. Kermoal JP, *et al*. Experimental investigation of correlation properties of MIMO radio channels for indoor picocell scenarios. In *IEEE VTC 2000-Fall*, Boston MA, U.S.A., September 2000.

DOI: 10.1002/wcm

30. Berrou C, Glavieux A, Thitimajshima P. Near shannon limit error-correcting coding and decoding: Turbo-codes. In *Proceedings of IEEE International Conference on Communications (ICC'93)*, Geneva, Switzerland, May 1993; 1064–1070.
31. Gallager R. *Low Density Parity Check Codes*. Cambridge, MIT Press, 1963
32. Chen J, Fossorier M. Near optimum universal belief propagation based decoding of low-density parity check codes. *IEEE Transactions on Communication* 2002; **50**(3): 406–E414.
33. Oien GE, Holm H, Hole KJ. Adaptive coded modulation with imperfect channel state information: system design and performance analysis aspects. In *Proceedings of IEEE International Symposium Advances in Wireless Communications*, Victoria, Canada, September 2002; 19–24.

Authors' Biographies

Wladimir Bocquet received the engineering degree and M.E. degree in communication engineering from ENST de Bretagne, Brest, France, and University of Rennes, Rennes, France, both in 2000. He joined Fujitsu Laboratories Ltd. in 2000. Since 2005, he has been with France Telecom R&D, Tokyo Laboratory, Tokyo, Japan. His research interests include digital signal processing for wireless communications. He is a member of IEEE.

Kazunori Hayashi received the B.E., M.E. and Ph.D. degrees in communication engineering from Osaka University, Osaka, Japan, in 1997, 1999 and 2002, respectively. Since 2002, he has been with the Department of Systems Science, Graduate School of Informatics, Kyoto University. He is currently an Assistant Professor there. His research interests include digital signal processing for communication systems.

Hideaki Sakai received the B.E. and D.E. degrees in applied mathematics and physics from Kyoto University, Kyoto, Japan, in 1972 and 1981, respectively. From 1975 to 1978, he was with Tokushima University. He is currently a Professor in the Department of Systems Science, Graduate School of Informatics, Kyoto University. He spent 6 months from 1987 to 1988 at Stanford University as a Visiting Scholar. His research interests are in the areas of adaptive and statistical signal processing. He served as an associate editor of *IEEE Transactions on Signal Processing* from January 1999 to January 2001.

DOI: 10.1002/wcm